

Running Head: Cytokinin-dependent protection of photosynthesis

Corresponding Author: Eduardo Blumwald

Department of Plant Sciences, University of California, One Shields Avenue, Davis, CA 95616.

Telephone number: +1 530 752 4640; **FAX:** +1 530 752 2278

Email: eblumwald@ucdavis.edu

Subject Area: Environmental and Stress Responses

Number of black and white figures, color figures and tables:

Black and white figures: 2

Color figures: 5

Supplementary black and white figures: 1

Supplementary color figures: 1

Supplementary tables: 11

© The Author 2010. Published by Oxford University Press on behalf of Japanese Society of Plant Physiologists. All rights reserved. For Permissions, please e-mail: journals.permissions@oxfordjournals.org

Title: Enhanced cytokinin synthesis in tobacco plants expressing $P_{SARK}::IPT$ prevents the degradation of photosynthetic protein complexes during drought.

Author's Full Names: Rosa M Rivero,¹ Jacinta Gimeno¹, Allen Van Deynze¹, Harkamal Walia² and Eduardo Blumwald^{1,*}

Institution Addresses:

¹Department Plant Sciences, University of California, Davis, CA 95616; ²Department of Agronomy and Horticulture, University of Nebraska, Lincoln, NE.

ABSTRACT

To identify genes associated with the cytokinin-induced enhanced drought tolerance, we analyzed the transcriptome of wild type and transgenic tobacco (*Nicotiana tabacum* 'SR1') plants expressing *P_{SARK}::IPT* (for Senescence-Associated Receptor Kinase::Isopentenyltransferase) grown under well-watered and prolonged water deficit conditions using the tomato GeneChip. During water deficit, the expression of genes encoding for the carotenoid pathway leading to ABA biosynthesis was enhanced in the wild-type plants, but repressed in the transgenic plants. On the other hand, transgenic plants displayed higher transcripts abundance of genes involved in the brassinosteroid biosynthetic pathways. Several genes coding for proteins associated with chlorophyll synthesis, the light reactions, Calvin-Benson cycle and photorespiration were induced in the transgenic plants. Notably, increased transcript abundance of genes associated with PSII, cyt b6/f complex, PSI, NADH oxidoreductase and ATP complex was found in the *P_{SARK}::IPT* plants. The increased transcript abundance was assessed by qPCR and the increased protein levels were confirmed by western blots. Our results indicated that while the photosynthetic apparatus in the wild-type plants was degraded, photosynthesis in the transgenic plants was not affected and photosynthetic proteins were not degraded. During water deficit, wild-type plants displayed a significant reduction in electron transfer and photochemical quenching with a marked increase in non-photochemical quenching, suggesting a decrease in energy transfer to the PSII core complexes and the increase in cyclic electron transfer reactions.

Keywords: *Nicotiana tabacum* 'SR1', cytokinins, drought, water deficit, photosynthesis, *IPT*.

INTRODUCTION

Water deficit imposes severe physiological and biochemical limitations to plant growth and productivity. During drought stress, a series of hormonal changes have been reported (such as decrease in CK, increase in ABA, etc.) (Davies and Zhang, 1991). These changes in hormone homeostasis due to water deficit typically lead to the inhibition of photosynthesis (Chaves 1991). The inhibition of photosynthetic activity under stress is due to a decrease in CO₂ availability caused by the limitation of CO₂ diffusion (Cornic, 2002; Flexas et al., 2007) and/or changes in the biochemical control of photosynthesis where RuBP synthesis, ATP synthesis, electron transfer, etc. are inhibited (Lawlor 2002, Rivero et al., 2009). Although during relatively mild water stress, stomatal limitations account for most of the decrease in photosynthesis, during more severe or prolonged drought stress the breakdown of the photosynthetic machinery is a major factor in the reduction of CO₂ assimilation (Tambussi et al., 2000). Of the several energy transducing complexes of the photosynthetic machinery, Photosystem II (PSII) is a critical multi-subunit complex composed of a core, the light-harvesting chlorophyll antenna (LHCII) and the oxygen-evolving complex (OEC). The core is comprised of the reaction centre proteins D₁ and D₂, the internal antenna proteins CP43 and CP47, cyt b₅₅₉ (Giardi et al., 1997) and the phosphoprotein TSP9 (Hansson et al., 2007). The PSII proteins D1-D2 form a heterodimer. This heterodimer is essential for initiating the transport of electrons liberated from the breakdown of H₂O and to produce energy (ATP) and reduced equivalents (NADPH) for CO₂ assimilation. The electrons are transferred from the D1-D2 heterodimer to the PSI through the cytochrome b6/f complex and eventually regenerate NADPH. The resulting proton gradient across the thylakoid membrane is used to generate ATP (Shikanai, 2007). This process, called linear electron transport (LET), is coupled to the cyclic electron

transport (CET) which comprises of PSI, ferredoxin (Fd) and the plastoquinone pool (PQ). During CET, the electrons are recycled from NAD(P)H or Fd to PQ to generate a proton gradient without NADPH accumulation (Shikanai, 2007). Although CET plays important roles in cyanobacteria, algae and C₄ plants, it is thought to have minimal influence in C₃ plants under steady state photosynthesis (Long et al., 2008). However, CET plays a significant role under environmental stress (Munekage et al., 2002; Nandha et al., 2007; Okegawa et al., 2008). During prolonged water deficit, the steady state levels of major PSII proteins decline, possibly because of the increased protein degradation and inhibition of protein synthesis (Aro et al., 1993; He et al., 1995). In addition, reactive oxygen species accumulate in the chloroplast inducing the damage of the thylakoid membranes and photoinhibition (Tambussi et al., 2000).

Hormones mediate the adaptation of plant growth and development to changing environmental conditions (Wolters and Jurgens, 2009) and extensive overlaps exist between drought-associated genes of plants in response to drought and gene expression in plants in response to hormones including ABA, auxins, CKs, gibberellic acid (GA), jasmonic Acid (JA) and Brassinosteroids (BRs) (Huang et al., 2009). However, while CK and ABA have been clearly associated with senescence and drought responses, respectively, the roles of other plant hormones such as GA, auxin, ethylene and BRs in the response of plants to water deficit are relatively less characterized. Nevertheless, a dynamic interaction among the various hormones, changing with development and tissue types at the same developmental stage, can be expected (Achard et al., 2006).

We have shown previously that stress-induced leaf senescence could be delayed in transgenic plants expressing isopentenyltransferase (IPT), an enzyme that catalyzes the rate-limiting step in CK synthesis under the control of SARK, a maturation- and stress-inducible promoter (Rivero et

al., 2007). Transgenic plants expressing $P_{SARK}::IPT$ grown under water deficit conditions displayed enhanced levels of CKs but did not show a consistent pattern for the steady state levels of ABA (Rivero et al., 2007). Increased CK production resulted in enhanced drought tolerance of the transgenic $P_{SARK}::IPT$ plants, with minimal yield loss (Rivero et al., 2007). Following a severe drought treatment, the production of CKs in transgenic plants expressing $P_{SARK}::IPT$ led to enhanced photosynthesis and improved water use efficiency (Rivero et al., 2007). When WT and transgenic $P_{SARK}::IPT$ tobacco (*Nicotiana tabacum* CV SR1) were grown under optimal or restricted (30% of optimal) watering regimes, there was no significant difference in stomatal conductance between leaves from WT or transgenic plants, but the WT plants displayed a significant reduction in the maximum rate of electron transport as well as the use of triose-phosphates suggesting a biochemical control of photosynthesis under long-term water deficit (Rivero et al., 2009). The transgenic plants growing under water deficit conditions, displayed a cytokinin-induced enhanced photorespiration that contributed in the protection of photosynthetic processes suggesting the beneficial role of photorespiration during drought (Rivero et al., 2009). Here we have used a large-scale expression profiling approach to investigate the effects of $P_{SARK}::IPT$ on gene expression to elucidate the molecular events associated with the CK-induced drought tolerance displayed by the $P_{SARK}::IPT$ plants. Our results show that during water stress, increased levels of CKs in the transgenic plants resulted in the transcriptional activation of chlorophyll biosynthesis and light reactions-related genes, a higher turnover of proteins associated with the photosynthetic apparatus and activation of genes associated with BR biosynthesis.

RESULTS AND DISCUSSION

Drought stress responsive genes in WT and $P_{SARK}::IPT$ plants

We have shown previously that transgenic plant expressing the *IPT* gene under the control of SARK, a stress- and senescence-induced promoter, displayed a remarkable tolerance when grown under reduced water regimes that inhibited the growth and yield of WT plants (Rivero et al., 2007, 2009). To identify genes associated with the CK-induced enhanced drought tolerance, we assayed and compared the transcriptomes of wild-type (WT) and $P_{SARK}::IPT$ plants growing under well-watered (1000 mLd⁻¹) and restricted watering conditions (300 mLd⁻¹) (Figure 1A). Because a microarray platform for *Nicotiana tabacum* was not available when these experiments were initiated, we used the EST-based tomato GeneChip from Affymetrix, representing ~9,200 transcripts, for heterologous hybridization. Roughly 41 % of the probe sets on the tomato array had a present call when processed RNA from *Nicotiana* was hybridized. The data generated was examined for quality, corrected for background and normalized as described in Materials and Methods. The differential expression analysis was performed using Statistical Analysis of Microarray (SAM) software. We used an arbitrary cut-off of 1 % false discovery rate (FDR) for identifying differentially expressed genes among samples. Most of the genes that fulfilled the stringent differential expression criteria were up- or down-regulated by at least a 2- or more fold change. Using the analysis described above we first sought to identify the differentially expressed genes in the two genotypes in response to 45 d of growth under water deficit conditions. A comparison between wild-type plants growing under well-watered and water deficit conditions identified 121 up-regulated probe sets and 322 probe sets down-regulated in response to water stress (Figure 1B; comparison 3, Supplemental Table S1 and S2). Similar stress triggered fewer transcript changes in $P_{SARK}::IPT$ plants (Figure 1B; comparison 4, Supplemental Table S3 and S4). Only 62 genes were up-regulated and 106 were down-regulated

in the transgenic plants grown under water deficient conditions. Our analysis suggested that the *P_{SARK}::IPT* plants experienced lower stress levels in agreement with the phenotypic characterization reported previously (Rivero et al., 2007, 2009). Next, we determined the extent of transcript-level conservation between the two genotypes in response to water deficit. Only 9 and 57 probe sets were up- and down-regulated, respectively in both genotypes. The comparison (between 3 and 4, Figure 1B) clearly indicated a diverged transcriptome response resulting from a direct or a downstream effect(s) by *P_{SARK}::IPT* expression. To ensure that the minimal overlap between the two genotypes was not a result of our stringent statistical cut-off, we performed the same comparison using a relatively relaxed threshold of 5 % FDR. Although the number of differentially expressed genes increased greatly, the overlap between comparisons 3 and 4 (Figure 1B) reflecting the conservation of transcript level responses was even lower. In summary, the drought stress responsive gene sets were markedly diverged in the transgenic plants expressing *P_{SARK}::IPT*. If the number of transcript changes in response to drought is considered a proxy for relative tolerance, this analysis indicated a less perturbed transcriptome of highly tolerant *P_{SARK}::IPT* plants.

Contrasting responses between the two genotypes during drought stress

We extended our analysis of the drought-responsive genes by attempting to identify genes that displayed a contrasting response to water deficit between the two genotypes. To this end, we searched for genes which were induced in *P_{SARK}::IPT* plants but repressed in WT plants during water deficit and found 7 genes (Supplemental Table S5). Notable among these there was an auxin responsive gene (LesAffx.71035.1.S1_at) that was induced in transgenic plants (1.8 fold, FDR 0%) but repressed in WT (2.3 fold, FDR 0%). The *Arabidopsis* Response dataset

(www.geneinvestigator.com; www.tair.org) indicated that the *Arabidopsis* ortholog of this gene (*At3g03840*) was strongly repressed by drought, ABA and high light but was activated by the phytohormones auxin, zeatin (a cytokinin) and brassinolide treatments. The induction of Les Affix.71035.1.S1_at expression in the transgenic plants would suggest an effect of increased CK possibly overriding an ABA effect (Suppl. Fig. 1). In addition, genes encoding for a chloroplast ATP synthase and a cytochrome f apoprotein also displayed expression trajectories parallel to the auxin responsive gene. A converse comparison i.e. for genes that were induced in WT during drought, but repressed in transgenic plants, yielded a null set.

Differential transcriptome regulation by increased CK levels

Our objective is to understand the shift in transcriptome dynamics associated with activation of the *P_{SARK}::IPT* gene, the production of CKs and the concomitant improved plant survival and growth during water deficit. To address this fundamental question on the role of CKs, we first compared the transcriptome of WT and transgenic *P_{SARK}::IPT* plants grown under well-watered conditions (Figure 1B; comparison 1, Supplemental Table S6 and S7). Using the defined statistical criteria described above, we identified 322 probe sets that were up-regulated and 393 were down-regulated in *P_{SARK}::IPT* plants as compared to WT plants. A parallel comparison for stressed plants (Figure 1B; comparison 2, Supplemental Table S8 and S9) indicated that 515 and 475 probe sets met the cutoff threshold for up- and down-regulation, respectively. The probe set numbers indicated that the transcriptomes of *P_{SARK}::IPT* and WT plants were strikingly different even under control conditions. The differences, as estimated from differentially expressed genes, became even larger upon the onset of water stress. We have shown previously that *IPT* was expressed under control conditions (Rivero et al., 2007). Further, we found that 216 probe sets

were commonly enriched and 203 probe sets were relatively repressed in the transgenic plants grown under well-watered and water restricted conditions. These results are surprising because under well-watered conditions, the WT and *P_{SARK}::IPT* plants did not display any phenotypic differences and physiological and biochemical characterization indicated similar levels of ROS detoxification and photosynthesis (Rivero et al., 2007, 2009).

To elucidate the role of CK in the tolerance to water deficit, we first examined the gene sets generated from the genotypic differential expression analyses. Several biological features emerged from the gene sets. Some of the salient features observed included a shift in certain hormone-associated pathways, activation of the tetrapyrrole biosynthesis pathways, starch metabolism associated genes and genes encoding photosynthetic electron transport components. While these features are notable and could explain the observed contrasting phenotypic differences between the *P_{SARK}::IPT* and WT plants, they are not an exhaustive coverage of the gene lists provided as supplementary data (Supplemental Table S1 to S9).

Distinct plant hormonal regulation in *P_{SARK}::IPT* plants

Plant hormones play important roles in almost all aspects of plant growth, development and their response to a multitude of environmental cues. Some of the well-studied hormones include auxins, CKs, GAs, ethylene, ABA, JA and BRs. The hormonal homeostasis that defines the physiological and developmental status of a plant is likely determined by the crosstalk among the different hormones. For instance, *JAZ1* is a protein that represses JA signaling pathways that was recently reported to be auxin inducible (Grunewald et al., 2009). Another instance of the antagonistic relationship among plant hormones was reported in *Arabidopsis*, where CK and IAA inhibit ABA-induced stomatal closure by enhancing ethylene production (Tanaka et al.,

2006). During drought stress the endogenous plant hormone levels change and these changes appear to impact grain yield and quality in wheat (Xie et al., 2003). Xie et al. (2003) demonstrated that changes in wheat yield and grain starch and protein content under drought were associated with reduced IAA, ZR and GA levels and the elevated ABA levels in plants, especially in grains. These and other reports highlight a shift in hormone levels in response to changing environment. In the *P_{SARK}::IPT* plants a gene encoding for *Gibberellin 20-oxidase1* (*GA20ox1*) was up-regulated by more than 8-fold (FDR 0%) relative to the WT plants (Figure 1B; comparisons 1 and 2). *GA20ox1* is involved in GA synthesis indicating that the increased CKs levels could promote increased transcription of GA synthetic pathways. The expression of the *Arabidopsis* ortholog of *GA20ox1* is strongly suppressed by water stress and to some degree by ABA treatments (www.geneinvestigator.com; www.tair.org). Interactions between CK and GA levels vary during plant development; high CK and low GA are required for shoot apical meristem (SAM) development, the site of active cell development (Jasinski et al., 2005). On the other hand, low CK and high GA signals are essential in mature and elongating cells (Yanai et al., 2005; Greenboim-Wainberg et al., 2005).

Repression of ABA-associated genes by increased CK

A gene coding carotenoid cleavage dioxygenase (NCED1) was induced in the WT plants but not in *P_{SARK}::IPT* plants (Rivero et al., 2009; Supplemental Fig. 1). The oxidative cleavage by NCED1 is considered to be the first committed and probably the rate regulating step in ABA biosynthesis downstream of the C₄₀ carotenoid pathway (Schwartz et al., 2003). Interestingly, the gene coding the upstream enzyme β -carotene hydroxylase, which converts β -carotene to zeaxanthin, was strongly repressed in the transgenic plants (Supplemental Figure 1; comparisons

1, 2). Further, the transcript abundance of violaxanthin de-epoxidase (NPQ1) was highly increased (7.8 fold, FDR 0 %) in the *P_{SARK}::IPT* plants relative to WT (Supplemental Figure 1). NPQ1 operates in the reverse direction (away from ABA biosynthesis) converting violaxanthin to antheraxanthin and zeaxanthin (Havaux and Nigoyi, 1999).

In addition to genes associated with ABA synthesis, we also found several genes encoding for ABA signaling components that were differentially regulated between the two genotypes (Supplemental Fig. 1). Among these, a protein phosphatase 2C (HAB2; homolog to ABI2) that was repressed in *P_{SARK}::IPT* plants. Also, the expression of *RCAR1* was repressed in the *P_{SARK}::IPT* plants relative to WT during stress. RCAR1 was shown recently to mediate the interaction between ABA and ABI2, the negative regulator of ABA responses (Ma et al., 2009). In general, the expression data indicated that ABA biosynthesis and ABA responsive genes were expressed at higher levels in the WT plants compared to the *P_{SARK}::IPT* plants (Supplemental Fig. 1).

P_{SARK}::IPT positively regulates the transcription of genes associated with BR biosynthesis.

BRs are hormones involved in plant growth and development, and mediate plant responses to the environment such as light and pathogen challenge (Bishop and Yokota, 2001). A comparison between WT and *P_{SARK}::IPT* plants showed a strong differential expression regulation in the early sterol biosynthetic pathway and its derivative hormone BR (Figure 3). FACKEL, SMT2, DWARF1 (DWF1), and cyclopropyl isomerase (CPI1), genes involved in sterol synthesis (Fujioka and Yokota, 2003), displayed higher transcript abundance in the transgenic plants compared to WT under both control and restricted water conditions. Several other genes involved in BR biosynthesis (e.g. BR-6-oxidase 1) and BR-signaling (BIN2) were also

differentially regulated. Almost all of the expression differences persisted between the WT and transgenic plants irrespective of the presence of stress, suggesting that the increased CK levels activated the transcription of genes associated with the biosynthesis of sterols and their derivative hormone. The positive interaction between CKs and BRs was further supported by a 2.3-fold up-regulation of cyclin D3 genes in transgenic plants. Cyclin D3 is a plant cyclin gene that mediates CK induced cell division that was reported to be induced by BR treatment (Hu et al., 2000; Mussig et al. 2002). Collectively, our data suggest that CKs activate BR biosynthesis and BR-activated pathways while negatively affecting the carotenoid pathway leading to ABA biosynthesis. The inter-hormonal interactions suggested by our data are consistent with the putative antagonism between ABA and CK, ABA and BR and the synergism between CK and BR (Wolters and Jurgens, 2009). An antagonistic relationship between ABA and CK has been postulated (Pospisilova and Dodd, 2005), and the expression of genes associated with ABA synthesis was repressed in *P_{SARK}::IPT* transgenic plants (Supplemental Fig. 1; Rivero et al., 2009), consistent with the increased CK content in the transgenic plants. Recently, the crosstalk between ABA and BR has been postulated (Zhang et al., 2009). It has been shown that the ABA and BR interaction requires the ABA signaling elements ABI1 and ABI2, as well as the BR-signaling component BIN2 (Zhang et al., 2009). Notably, the expression of HAB1 and HAB2, homologs of ABI1 and ABI2, respectively, was relatively higher in WT plants (Supplemental Fig. 1), while the expression of BIN2 was higher in the transgenic plants (Fig. 2), thus supporting an antagonistic relationship between ABA and BR. Although our data suggest an interaction between CK and BR, whether this interaction is direct, or indirectly mediated by ABA is not clear.

Increased endogenous CK results in transcriptional activation of chlorophyll biosynthesis

Transgenic plants expressing *P_{SARK}::IPT* maintained a higher photosynthetic activity during drought (Rivero et al., 2009). Consistent with this observation we found the transcriptional activation of several genes encoding for enzymes involved in chlorophyll biosynthesis in the transgenic plants (Figure 3). Some of them (for instance porphobilinogen deaminase and protochlorophyllide oxidoreductase, among others) displayed higher relative expression in *P_{SARK}::IPT* plants irrespective of the watering regimes. However, the expression of a gene coding for glutamyl-tRNA reductase, which has a role during early stages of tetrapyrrole synthesis was repressed in the WT plants during growth under water deficit but remained unchanged in the transgenic plants. Interestingly, the expression of genes encoding for Mg protoporphyrin chelatase (*MgCh*) was at least 2-fold higher in the WT plants relative to transgenic plants grown under controls conditions, and no significant expression difference was detected between the genotypes growing under water deficit. Magnesium chelatase catalyzes the first committed step in chlorophyll synthesis and is also considered to be an important component of the regulatory mechanism for chlorophyll synthesis (Rissler et al., 2002). In addition to its role in chlorophyll biosynthesis, the *Arabidopsis* ortholog of MgCh, *genomes uncoupled 5* (*GUN5*) has also been proposed to play an important role in plastid-to-nucleus signaling as well as ABA signaling (Mochizuki et al., 2001; McCourt and Creelman, 2008). Furthermore, plants over-expressing the major subunit of MgCh were reported to be hyper-sensitive to ABA, whereas knockout mutants showed ABA-insensitivity. The *GUN5* expression was strongly repressed by ABA and drought in the *Arabidopsis* expression atlas dataset (www.arabidopsis.org) and the potential regulatory role of MgCh in the context of CK-mediated chlorophyll biosynthesis during water stress should be further investigated.

Transcriptional activation of the light reactions-related genes under water deficit

Genes that were differentially expressed in WT and *P_{SARK}::IPT* plants grown under water deficit were imported into MapMan (<http://mapman.gabipd.org>) to obtain a transcriptional overview of the pathways that could be differentially regulated by CK. This analysis indicated that several genes coding proteins associated with the light reactions, Calvin-Benson cycle and photorespiration were up-regulated in the *P_{SARK}::IPT* transgenic plants (Figure 4, Supplemental Table S8 and S9). Notably, we found increased transcript abundance for genes associated with PSII, PSI, NADH oxidoreductase and ATPase complexes in *P_{SARK}::IPT* plants (Figure 5A). The expression of most of the photosynthesis-related genes listed was repressed in the WT, but induced in the *P_{SARK}::IPT* plants in response to water deficit (Fig. 5A). We further assayed the expression of a subset of these genes using qPCR (Figure 5B). All of the 16 genes tested were down-regulated in the WT and 15 of these genes had higher expression in *P_{SARK}::IPT* plants in response to water deficit.

We also tested the protein levels of several of the photosynthetic complex proteins in WT and *P_{SARK}::IPT* plants under control and water deficit conditions (Figure 6). The PSII reactions center proteins, D1 and D2 bind to electron transfer prosthetic groups such as P680, and plastoquinone. At the protein level, the expression of D1 was significantly reduced in WT plants under stress. However, the *P_{SARK}::IPT* plants maintained a higher level of D1 irrespective of soil moisture status (Fig. 6). The protein levels of D2 did not change significantly in the WT plants under stress, but displayed a slight increase in the *P_{SARK}::IPT* plants in response to water deficit. During water deficit conditions, the phosphorylation index of the PSII proteins increased and a reorganization of the photosystems occurred (Giardi et al., 1995). D1 levels have been reported

to be more sensitive to long-term drought stress in pea seedlings (Giardi et al., 1995) and a high rate of D1 protein turnover was shown to stabilize thylakoid membranes and the electron transport chains against oxygen free radicals that accumulate under water deficit (Guseynova et al., 2006). A similar expression pattern was seen with antibodies raised against OEC (Oxygen Evolving Complex) of PSII, cytochrome f of the cytochrome b6/f complex, PsaB (core protein of PSI) and α ATPase subunit with decreased protein levels in the WT plants exposed to water deficit, but unchanged and sometimes increased protein levels in the *P_{SARK}::IPT* plants (Fig. 6). Cyt b/6f complex-related genes encode for proteins that transfer electrons between the two reaction center complexes (PSI and PSII). They also participate in the formation of the transmembrane electrochemical proton gradient by transferring protons from the stroma to the internal lumen compartment. Senescence and stress lead to the degradation of the photosynthetic apparatus and the cyt b/6f complex (Hortensteiner, 2009), and the relatively stable protein levels seen in the transgenic plants grown under water deficit could be a consequence of the CK-induced delayed senescence observed in the transgenic plants (Rivero et al., 2007).

In contrast to the other photosynthesis-related protein tested, Ferredoxin (Fd) protein levels increased in the WT plants grown under water deficit (Fig. 6), and a similar increase was seen in the transgenic plants grown under water deficit. During stress, the energy that is not used to drive photosynthesis is dissipated as heat to avoid the generation of reactive oxygen species. In this situation, Fd drives the cyclic electron transfer (CET) reactions avoiding damage to PSI (Arnon et al., 1954). Using chlorophyll fluorescence measurements of WT and *P_{SARK}::IPT* plants, we determined the electron transport rate carried out by cyt b6/f complex (ETR) and the energy driven to photosynthesis (photochemical quenching, qP) or dissipated as heat (non-photochemical quenching, NPQ) (Fig. 7). Under well-watered conditions, no significant

differences were observed between WT and transgenic plants. However, during water deficit the WT plants displayed a marked reduction in ETR and qP, and an increase in NPQ (Fig. 7). The decrease in D1 protein levels and OEC in WT plants (Fig. 6), together with the reduction in ETR and qP and the increase in NPQ suggest a decrease in energy transfer to the PSII core complexes and a possible increase in CET during water deficit. In spite of the decrease in PsaB protein content and PsaN and PsaH gene expression, the increase in PSI activity (Supplemental Table S11) seen in WT plants during stress would suggest an increase in CET and would support the notion of a role of CET as a source of ATP for C3 plants under stress conditions, where CO₂ or RuBP can be limiting (Golding and Johnson, 2003; Nandha et al., 2007). The occurrence of CET in the WT plants during water deficit was also supported by the enhanced expression of *PGR5* (PROTON GRADIENT REGULATION 5). *PGR5* have been shown to be important for the activity of Fd-dependent CET (Munekage et al., 2008; Long et al., 2008). Although *P_{SARK}::IPT* plants also displayed an increase in Fd protein levels during water deficit (Fig. 6) and a relatively higher PSI activity (Supplemental. Table S11), these plants did not show an increase in NPQ or a decrease in qP or increased *PGR5* transcription during water deficit. Moreover, *P_{SARK}::IPT* plants displayed increased RuBP regeneration capacity during water deficit (Rivero et al., 2009). These results would suggest that the increased Fd levels during water deficit are not likely related to increased CET levels in the transgenic plants. The increase in Fd levels in *P_{SARK}::IPT* plants during water deficit cannot be explained within the frame of this study and requires further investigation.

In conclusion, during water deficit, wild-type plants activated ABA biosynthesis and ABA signaling pathways, a typical drought stress response. On the other hand, increased CK levels in

the transgenic plants expressing *P_{SARK}::IPT* resulted in the activation of BR synthesis and BR signaling and in the repression of drought-induced ABA responses. Recent reports have indicated that the treatment of plants with 24-epibrassinolide (an active BR) increased CO₂ assimilation and quantum yield of PSII in *Cucumis sativa* (Xia et al., 2009), and BR pretreatment protected PSII in *Vicia faba* treated with an herbicide (Pinol and Simon, 2009). This notion is supported by the data presented here. Taken together, the transcriptome analyses suggest that the prevention of the degradation of the photosynthetic protein complexes, and the maintenance of photosynthesis during prolonged water deficit in the transgenic *P_{SARK}::IPT* plants resulted in the activation of BR-associated pathways. Whether the activation of BR-associated genes was directly affected by CK or indirectly affected by the negative interaction between CK and ABA is not clear and is presently under investigation.

MATERIALS AND METHODS

Experimental Design

Seeds of wild-type tobacco (*Nicotiana tabacum* ‘SR1’) and transgenic plants expressing $P_{SARK}::IPT$ were sown in soil (Metro-Mix 200; Sun Gro) in a growth chamber (500 $\mu\text{mol photons m}^{-2} \text{ s}^{-1}$, 16-h photoperiod, 25°C) for 15 d until the emergence of the first two true leaves. Initially, 5 seeds/pot were germinated in the growth chamber. Fifteen days after germination, plants with two true leaves of similar size were chosen and 1 plant/pot was selected for experiments and continuously grown. During this period, no differences in germination rate and development between the wild type and $P_{SARK}::IPT$ were observed. Fifty plants of each genotype were transferred and transplanted (10-L pots) to a greenhouse, where they were grown for 1 week to allow acclimation of the plants to the new conditions (1,000 $\mu\text{mol photons m}^{-2} \text{ s}^{-1}$, 16-h photoperiod, 28°C–30°C/23°C–25°C day/night). At this point, half of the wild-type plants and half of the $P_{SARK}::IPT$ plants were selected to receive 1,000 mL of water per day (the amount of water necessary for tobacco plants to maintain cell turgor, designated as optimal watering conditions) (Rivero et al., 2007), whereas the other half of the plants received 300 mL of water per day (restricted watering regime). This amount of water was considered to induce water deficit, because it produced a 50% yield reduction in the wild-type plants (Rivero et al., 2007). For the transcriptome analyses, plants were grown for 45 d under a restricted watering regime. For physiological measurements, we used plants that were grown during 70 d at 300 mL per d. No water was allowed to drain from pots in any of the treatments. For microarray analysis, as well as for physiological and biochemical measurements, leaves at position 7th and 8th (corresponding to leaves at middle position) from WT and $P_{SARK}::IPT$ plants were harvested. The

expression profile of *IPT* was taken into consideration for the selection of these particular leaves positions (see Rivero et al., 2007). At day 67th, WT and transgenic plants did not show any sign of natural senescence and all the leaves collected at positions 7th and 8th were green. *IPT* expression profiles and CK contents of these leaves have been reported previously (Rivero et al., 2007; Rivero et al., 2009)

RNA preparation and GeneChip hybridization

RNA extraction, purification, labeling and hybridization to GeneChips was performed using standard protocols. Briefly, total RNA was isolated from leaf tissue using the TRIzol reagent. The RNA was cleaned by passing through an RNAeasy spin column (Qiagen, Chatsworth, CA). To eliminate traces of DNA, the RNA was treated with DNaseI (Fermentas Life Sciences, Honover, MD, EN0531) according to manufacturer's protocol. The RNA quality was assessed using the RNA Lab-On-A-Chip (Caliper Technologies Corp., Mountain View, CA) on a Agilent Bioanalyzer 2100 (Agilent Technologies, Palo alto, CA). A total of 2 µg of total RNA was used for each sample. Further labeling and hybridization steps were performed as recommended by Affymetrix, Inc. (Affymetrix Genechip Expression Analysis Technical Manual, Affymetrix, INC., Santa Clara, CA). Each biological replicate was hybridized to an array to obtain a total of 3 replicates for each genotype and treatment.

Real time quantitative PCR

cDNAs were obtained from two independent RNAs (2 µg of total RNA) using the SuperScript VILO cDNA synthesis kit (Invitrogen). The tissue materials were obtained from wild-type plants and *P_{SARK}::IPT* plants growing under control (1,000 mL d⁻¹) and water deficit (300 mL d⁻¹)

conditions. Every sample was represented by two independent cDNAs. The RNA used in the qPCR assays was obtained from the same pool that was used for array hybridizations.

From each cDNA, three technical replicates were used, so that every sample was represented by six replicates in total. ABI Primer Express software was used for primer design. The genes assayed for expression and the primer sequence used are listed in Supplemental Table 10.

Two independent internal controls (*18S* rRNA and *Ubiquitin-Conjugated Protein2* [*UBQ2*]), whose expression did not change across different samples were used. A total reaction volume of 20 μ L was used. Reactions included 2 μ L of template, 10 μ L of Fast SYBR Green Master Mix, 0.9 μ L of reverse primer, 0.9 μ L of forward primer, and sterile molecular biology-grade water to a total volume of 20 μ L. PCR assays were performed using the following conditions: 95°C for 10 min followed by 40 cycles of 95°C for 3 s and 60°C for 30 s. A melt curve analyses for all targets included the following conditions: 95°C for 15 s, 60°C for 1 min, and 95°C for 15 s. Amplification and data analysis were carried out using the ABI StepOne Plus real-time PCR system (Applied Biosystems) using internal controls *18S* rRNA and/or *UBQ2*. The relative fold change was measured against the control wild-type samples.

Thylakoid membrane isolation

Intact chloroplasts were isolated from wild-type and *P_{SARK}::IPT* tobacco plants. Twenty grams of leaves (same leaves used for thylakoid membrane isolation and DNA microarrays) were cut into small pieces and homogenized in a blender (3 x 5s) with 100 ml of grinding buffer containing 50 mM potassium phosphate (pH 7.5), 100 mM NaCl, 1mM MgCl₂, 1mM MnCl₂, 300 mM sorbitol, 10 mM potassium ascorbate, 2mM EDTA and 50 mM HEPES buffer (pH 7.5). The resulting homogenate was filtered through Miracloth and the homogenate centrifuged at 200 xg for 2 min.

The supernatant was then centrifuged at 5000 $\times g$ for 10 min and the pellet resuspended in 15 ml of a wash buffer containing 50 mM potassium phosphate (pH 7.5), 50 mM NaCl, 1mM $MgCl_2$, 1mM $MnCl_2$ and 300 mM sorbitol. The suspension was centrifuged at 200 $\times g$ for 2 min and the supernatant centrifuged at 5000 $\times g$ for 10 min. The pellet was resuspended in 1-2 ml of the same medium. Isolated chloroplast were osmotically shocked by a 10-fold dilution with 50 mM potassium phosphate buffer (pH 7.5), 10 mM NaCl and 1 mM $MgCl_2$ and incubation in ice for 3 min. After centrifugation at 5000 $\times g$ for 5 min the thylakoid pellet was washed with the same buffer and centrifuged again under the same conditions. The pellet was resuspended in 1-2 ml of washing buffer. Chlorophyll concentration was calculated with 80% acetone as described by Arnon (1949). All procedures were carried out at 4°C and preparations were protected from light. The isolated thylakoid membranes were used for photosynthetic activity measurements or for western blots within the next 2 hours after isolation.

Immunoblotting.

For western blots, thylakoid membranes from frozen leaves (same leaves used for thylakoid membrane isolation and DNA microarrays) were used. Thylakoid membrane isolation from frozen tissue was achieved according to Rintamäki *et al.* (1996) with some modifications; frozen leaves were homogenized in a mortar with liquid nitrogen and ice-cold isolation buffer containing 50 mM HEPES-NaOH, pH 7.5, 300 mM sucrose, 5 mM $MgCl_2$, 1 mM Na-EDTA, 10 mM NaF, and 1 % (m/v) bovine serum albumin. The homogenates were filtered through Miracloth and centrifuged at 1500 $\times g$ for 4 min. The pellets were washed with 10 mM HEPESNaOH (pH 7.5), 5 mM sucrose, 5 mM $MgCl_2$, and 10 mM NaF, and centrifuged at 3000 $\times g$ for 3 min. Thylakoid pellets were re-suspended in assay buffer consisting of 50 mM Hepes-

NaOH (pH 7.5), 100 mM sucrose, 5 mM NaCl, 10 mM MgCl₂, and 10 mM NaF at a final Chl concentration of 0.4 kg m⁻³. The isolated thylakoid membranes were immediately used for the western blots. The preparations were protected from light and kept ice-cold during the isolation procedure. The isolated thylakoids were solubilized in 0.5 M Tris-HCl (pH 6.8), 7 % SDS, 20 % glycerol, and 2 M urea, and then incubated at 100 °C for 5 min. Non-solubilized materials were removed by centrifugation at 8000 ×g for 8 min. SDS-PAGE was made according to Laemmli *et al.* (1970) using 14 % (w/v) acrylamide, and 6 M urea. Each sample contained 0.5 µg Chl. Chl was extracted with 80 % acetone solution and determined spectrophotometrically as described by Porra *et al.* (1989). For immunoblotting the proteins were transferred to a polyvinylidene difluoride membrane (PVDF) (Immun-Blot; Bio-Rad, Hercules, CA, USA). The membranes were then blocked with 5% fat-free milk, incubated with the primary antibody (PsaA, PsaB, D1,D2, cytb6/f, Fd, cyt b559, OEC, or ATPase-alpha subunit). Antibodies were obtained from AGRISERA AB (Sweden) and used at recommended dilutions. Membranes were washed 3 times for 10 min in TBST, immunostained with polyclonal rabbit antibodies and visualized using enhanced chemiluminescence (ECL; Amersham Biosciences Ltd, Bucks., UK).

Measurement of PSI activity

Photosynthetic oxygen uptake rates were determined using a Clark-type oxygen electrode (Hansatech, King's Lynn, UK). The reaction mixture (2ml) contained: 330 mM sorbitol, 40mM Tricine buffer (pH 7.6), 2 mM EDTA, 7 mM MgCl₂ and 30 µg of thylakoid membranes. This suspension was incubated in the darkness for 3 min. The temperature of the vessel containing the suspension was maintained constant at 25°C. PSI activity was measured in the presence of 0.2 mM tetramethyl-p-phenylenediamine (TMPD), 3mM ascorbate, 0.1 mM methyl viologen (MV),

15 μM 3-(3,4-dichlorophenyl)-1,1-dimethylurea (DCMU) and 5mM NaN_3 (Romanowska, 2006) under a light intensity of $1200 \mu\text{mol m}^{-2} \text{s}^{-1}$.

Fluorescence measurements

Measurements of chlorophyll fluorescence were performed on the 8th leaf of WT and transgenic plants by using a portable fluorometer (LI-6400-40, LICOR Biosciences, Lincoln, USA). The maximal photochemical efficiency of PSII was estimated by the fluorescence ratio F_v/F_m calculated from F_o (basal fluorescence) and F_m (maximal fluorescence), with F_v being the variable fluorescence. The intrinsic efficiency of open PSII reaction centers (F_v'/F_m' ratio) was calculated by measuring the same parameters as above, but under natural irradiance (F_o' and F_m'). After the saturating flash of 0.8 sec and the determination of F_m' and F_s (steady-state fluorescence), a black cloth was placed over the leaf for 20 min and a far-red pulse of 3 s was applied to fully oxidizes PSII during F_o' measurement. The photochemical efficiency of PSII in light-adapted leaves (ψ_{PSII}) was calculated by the $F_m' - F_s'/F_m' = \Delta F/F_m'$ ratio (Genty et al., 1989). The photochemical quenching (qP), which was used as an estimate of the fraction of open reaction centers, was calculated as the ratio: $qP = 1 - (F_s - F_o')/(F_m' - F_o')$ (Bilger and Schreiber, 1986). The thermal energy dissipation or non-photochemical quenching (NPQ) at the PSII level was estimated by using the Stern–Volmer equation: $\text{NPQ} = (F_m/F_m') - 1$ (Cornic, 1994). The electron transport rate (ETR) was estimated as described by Krall and Edwards (1992): $\Delta F/F_m' \times \text{PPFD} \times 0.5 \times 0.84$. We used the common C3 leaf absorbance value of 0.84 (Bjorkman and Demmig, 1987).

Statistical Analysis

Scanned GeneChip images were examined for visual aberrations. All the images obtained were of high quality. Further preprocessing and analysis was performed using the .CEL files. The .CEL files were imported into RMA [Irizarry et al., 2003] for further processing. The background adjustment and quantile normalization were performed using the default settings. The log-transformed values from RMA were imported into Significance Analysis of Microarrays (SAM) software [Tusher et al., 2001]. To perform differential expression analysis we used the two-class unpaired selection in SAM. The test statistics used was the T-statistic. The arbitrary cut-off for calling differential expression was set at 1% FDR (q-value). We did not use a fold change threshold for analysis using SAM. However, majority of the genes with identified at 1 % FDR were differentially regulated by more than 2-fold.

Unsupervised hierarchical clustering analysis was performed using the normalized probeset expression values. The threshold for calling significant gene clusters was set to a p -value ≥ 0.001 . Pearson correlation was used for placing neighboring probe sets.

Data availability

All microarray data from this work are available from NCBI GEO (www.ncbi.nlm.nih.gov/geo) under the series entry GSE19787.

FUNDING.

This research was supported by a grant from the UC Discovery Program, Arcadia Biosciences Inc, and the Will W. Lester Endowment, University of California, Davis.

REFERENCES

- Archard, P., Cheng, H., De Grauwe, L., Decat, J., Schoutteten, H., Moritz, T., et al. (2006) Integration of plant responses to environmentally activated phytohormonal signals. *Science* 311: 91-94
- Arnon, D.I. (1949) Cooper enzymes in isolated chloroplasts and polyphenol oxidase in *Beta vulgaris*. *Plant Physiol* 24:1-15
- Arnon, D.I., Allen, M.B. and Whatley, F.R.(1954) Photosynthesis by isolated chloroplasts. *Nature* 174: 394-396
- Aro, E.M., McCaffery, S. and Anderson, J.M. (1993) Photoinhibition and D1 protein degradation in peas acclimated to different growth irradiances. *Plant Physiol* 103: 835-843
- Bilger, W. and Schreiber, U. (1986) Energy-dependent quenching of dark level chlorophyll fluorescence in intact leaves. *Phot Res* 10: 303-308.
- Bishop, G.J. and Yokota, T. (2001) Plant steroid hormones, brassinosteroids: current highlights of molecular aspects on their synthesis, metabolism, transport, perception and response. *Plant Cell Physiol* 42: 114-120
- Björkman, O. and Demmig, B. (1987) Photon yield of O₂ evolution and chlorophyll fluorescence characteristics at 77K among vascular plants of diverse origins. *Planta* 170: 489-504.
- Chaves, M.M. (1991) Effects of water deficits on carbon assimilation. *J Exp Bot* 42: 1-16
- Cornic, G. (1994) Drought stress and high light effects on leaf photosynthesis. In: Baker, NR, Bowyer, JR (Eds.), *Photoinhibition of Photosynthesis: From Molecular Mechanisms to the Field*. BIOS Scientific Publishers, Oxford, pp. 297-313.
- Cornic, G. (2002) Drought stress inhibits photosynthesis by decreasing stomatal aperture: not by affecting ATP synthesis. *Tr Plant Sci* 5: 187-188
- Davies, W.J. and Zhang, J.H. (1991) Root signal and the regulation of growth and development of plants in drying soil. *Annu Rev Plant Physiol Plant Mol Biol* 42: 55-76

Flexas, J., Diaz-Espejo, A., Galme's, J., Kaldenhoff, R., Medrano, H. and Ribas-Carbo, M. (2007) Rapid variations of mesophyll conductance in response to changes in CO₂ concentration around leaves. *Plant Cell Env* 30: 1284-1298.

Fujioka, S. and Yokota, T. (2003) Biosynthesis and metabolism of brassinosteroids. *Annual Review of Plant Biology* 54: 137-164

Genty, B., Briantais, J.M. and Baker, N.R. (1989) The relationship between the quantum yield of photosynthetic electron transport and quenching of chlorophyll fluorescence. *Biochim Biophys Acta* 990: 87-92.

Giardi, M.T., Cona, A., Geiken, B., Kucera, T., Masojidek, J. and Mattoo, A.K. (1995) Long term drought stress induces structural and functional reorganization of photosystem II. *Planta* 199: 118-125

Giardi, M.T., Masojidek, J. and Godde, D. (1997) Effects of abiotic stresses on the turnover of the D-1 reaction centre II protein. *Physiol Plant* 101: 635-642

Golding, A.J. and Johnson, G.N. (2003) Down-regulation of linear and activation of cyclic electron transport during drought. *Planta* 218: 107-114

Greenboim-Wainberg, Y., Maymon, I., Borochoy, R., Alvarez, J., Olszewski, N., Ori, N., et al. (2005) Cross talk between gibberellin and cytokinin: the Arabidopsis GA-response inhibitor SPINDLY plays a positive role in cytokinin signaling. *Plant Cell* 17: 92-102

Grunewald, W., Vanholme, B., Pauwels, L., Plovie, E., Inze, D., Gheysen, G., et al. (2009) Expression of the Arabidopsis jasmonate signaling repressor JAZ1/TIFY10A is stimulated by auxin. *EMBO Rep* 10: 923-928

Guseynova, I.M., Suleymanov, S.Y. and Aliyev, J.A. (2006) Protein composition and native state of pigments of thylakoid membrane of wheat genotypes differently tolerant to water stress. *Biochemistry-Moscow* 71: 173-177

Hansson, M., Dupuis, T., Stromquist, R., Andersson, B., Verner, A.V. and Carlberg, I. (2007) The mobile thylakoid phosphoprotein TSP9 interacts with the Light-Harvesting Complex II and the peripheries of both photosystems. *J Biol Chem* 282: 16214-16222.

Havaux, M. and Niyogi, K. (1999) The violaxanthin cycle protects plants from photooxidative damage by more than one mechanism. *Proc Natl Acad Sci USA* 96: 8762-8767

He, J.X., Wang, J. and Liang, H.G. (1995) Effects of water-stress on photochemical function and protein metabolism of photosystem II in wheat leaves. *Physiol Plant* 93: 771-777

Hortensteiner, S. (2009) Stay-green regulates chlorophyll and chlorophyll-binding protein degradation during senescence. *Tr Plant Sci* 14: 155-162

Hu, Y., Bao, F. and Li, J. (2000) Promotive effect of brassinosteroids on cell division involves a distinct CycD3-induction pathway in *Arabidopsis*. *Plant J* 24: 693-701

Huang, D., Wu, W., Abrams, S.R. and Cutler, A.J. (2009) The relationship of drought-related gene expression in *Arabidopsis thaliana* to hormonal and environmental factors. *J Exp Bot* 59: 2991-3007

Irizarry, R.A., Hobbs, B., Collin, F., Beazer-Barclay, Y.D., Antonellis, K.J., Scherf, U., et al. (2003) Exploration, normalization, and summaries of high density oligonucleotide array probe level data. *Biostatistics* 4: 249-264

Jasinski, S., Piazza, P., Craft, J., Hay, A., Woolley, L., Rieu, I., et al. (2005) KNOX action in *Arabidopsis* is mediated by coordinate regulation of cytokinin and gibberellin activities. *Curr Biol* 15:1560-1565

Laemli, U.K. (1970) Cleavage of structural proteins during the assembly of the head of bacteriophage T4. *Nature* 227 680-685

Lawlor, D.W. (2002) Limitation to photosynthesis in water-stressed leaves: stomata vs. metabolism and the role of ATP. *Ann Bot (Lond)* 89: 871-885

Lichtenthaler, H.K. (1987) Chlorophylls and carotenoids: Pigments of photosynthetic membranes. *Meth Enzymol* 148:350-382

Long, T.A., Okegawa, Y., Shikanai, T., Schmidt, G.W. and Covert, S.F. (2008) Conserved role of PROTON GRADIENT REGULATION 5 in the regulation of PSI cyclic electron transport. *Planta* 228: 907-918

Ma, Y., Szostkiewicz, I., Korte, A., Moes, D., Yang, Y., Christman, A., et al. (2009) Regulators of PP2C phosphatase activity function as abscisic acid sensors. *Science* 324: 1064-1068

McCourt, P. and Creelman, R. (2008) The ABA receptors – we report you decide. *Curr Op Plant Biol* 11: 474-478

Mochizuki, N., Brusslan, J.A., Larkin, R., Nagatani, N. and Chory, J. (2001) Arabidopsis genomes uncoupled 5 (GUN5) mutant reveals the involvement of Mg-chelatase H subunit in plastid-to-nucleus signal transduction. *Proc Natl Acad Sci USA* 98: 2053-2058.

Munekage, Y., Hojo, M., Meurer, J., Endo, T., Tasaka, M. and Shikanai, T. (2002) PGR5 is involved in cyclic electron flow around photosystem I and is essential for photoprotection in Arabidopsis. *Cell* 110: 361-371

Munekage, Y.N., Genty, B. and Peltier, G. (2008) Effect of PGR5 Impairment on Photosynthesis and Growth in Arabidopsis thaliana. *Plant Cell Physiol* 49: 1688-1698

Mussig, C. (2005) Brassinosteroid-promoted growth. *Plant Biol* 7: 110-117

Nandha, B., Finazzi, G., Joliot, P., Hald, S. and Johnson, G.N. (2007) The role of PGR5 in the redox poisoning of photosynthetic electron transport. *Biochim Biophys Acta* 1767: 1252-1259

Okegawa, Y., Long, T.A., Iwano, M., Takayama, S., Kobayashi, Y. and Covert, S.F. (2007) A balanced PGR5 level is required for chloroplast development and optimum operation of cyclic electron transport around photosystem I. *Plant Cell Physiol* 48: 1462-1471

Okegawa, Y., Kagawa, Y., Kobayashi, Y. and Shikanai, T. (2008) Characterization of factors affecting the activity of photosystem I cyclic electron transport in chloroplasts. *Plant Cell Physiol* 49: 825-834

Piñol, R. and Simon, E. (2009) Effect of 24-Epibrassinolide on chlorophyll fluorescence and photosynthetic CO₂ assimilation in *Vicia faba* plants treated with the photosynthesis-inhibiting herbicide terbutryn. *J Plant Growth Regul* 28: 97-105

Porra, R.J., Thompson, W.A. and Kriedemann, P.E. (1989) Determination of accurate extinction coefficients and simultaneous equations for assaying chlorophyll A and chlorophyll B extracted with 4 different solvents. Verification of the concentration of chlorophyll standards by atomic absorption spectroscopy. *Biochim Biophys Acta* 975: 384-394

Pospisilova, J. and Dodd, I.C. (2005) Role of plant regulators in stomatal limitation of photosynthesis during water stress. In M Pessaraki, ed. Handbook of Photosynthesis, Ed 2, Revised and Expanded. Marcel Dekker, New York, pp 811-825

Rivero, R.M., Kojima, M., Gepstein, A., Sakakibara, H., Mittler, R., Gepstein, S. et al. (2007) Delayed leaf senescence induces extreme drought tolerance in a flowering plant. *Proc. Natl. Acad. Sci. USA* 104: 19631-19636

Rivero, R.M., Shulaev, V. and Blumwald, E. (2009) Cytokinin-Dependent photorespiration and the protection of photosynthesis during water deficit. *Plant Physiol* 150: 1530-1540

Rissler, H.M., Collakova, E., DellaPenna, D., Whelan, J. and Pogson, B.J. (2002) Chlorophyll Biosynthesis expression of a second *Chl I* gene of magnesium chelatase in Arabidopsis supports only limited chlorophyll synthesis. *Plant Physiol* 128: 770-779

Romanowska, E., Drozak, A., Pokorska, B., Shiell, B.J. and Michalski, W.P. (2006) Organization and activity of photosystems in the mesophyll and bundle sheath chloroplasts of maize. *J Plant Physiol* 163: 607-610

Shikanai, T. (2007) Cyclic electron transport around Photosystem I: Genetic approaches. *Annu Rev Plant Biol* 58: 199-217

Schwartz, S.H., Qin, X. and Zeevaart, J.A.D. (2003) Elucidation of the indirect pathway of abscisic acid biosynthesis by mutants, genes, and enzymes. *Plant Physiol* 131: 1591-1601

Tambussi, E.A., Bartoli, C.G., Beltrano, J., Guiamet, J.J. and Araus, J.L. (2000) Oxidative damage to thylakoid proteins in water-stressed leaves of wheat (*Triticum aestivum*). *Physiol Plant* 108: 398-404

Tanaka, M., Takei, K., Kojima, M., Sakakibara, H. and Mori, H. (2006) Auxin controls local cytokinin biosynthesis in the nodal stem in apical dominance. *Plant J* 45:1028-1036

Tusher, V.G., Tibshirani, R. and Chu, G. (2001) Significance analysis of microarrays applied to the ionizing radiation response. *Proc Natl Acad Sci USA* 98: 5116-5121

Wolters, H. and Jurgens, G. (2009) Survival of the flexible: hormonal growth control and adaptation in plant development. *Nature Gen* 10: 305317

Xia, S.J., Huang L.F., Zhou Y.H., Mao W.H., Shi K., Wu J.X., et al. (2009) Brassinosteroids promote photosynthesis and growth by enhancing activation of Rubisco and expression of photosynthetic genes in *Cucumis sativus*. *Planta* 230:1185-1196

Xie, Z.J., Jiang, D., Cao, W.X., Dai, T.B. and Jing, Q. (2003). Relationships of endogenous plant hormones to accumulation of grain protein and starch in winter wheat under different post-anthesis soil water statuses. *Plant Growth Regul.* 41, 117-127.

Yanai, O., Shani, E., Dolezal, K., Tarkowski, P., Sablowski, R., Sandberg, G., et al. (2005) Arabidopsis KNOXI proteins activate cytokinin biosynthesis. *Curr Biol* 15: 1566–1571

Zhang, S., Cai, Z. and Wang, X. (2009) The primary signaling outputs of brassinosteroids are regulated by abscisic acid signaling. *Proc Natl Acad Sci USA* 106: 4543-4548

LEGEND TO FIGURES

Figure 1. Experimental design and differential expression comparisons. (A) Scheme of the experimental design and time points at which the samples were collected for expression analysis (indicated by green ovals). The green broken line indicates daily watering (1000 mLd^{-1}) of WT and $P_{\text{SARK}}::\text{IPT}$ transgenics plants. The blue line represents both genotypes under limited water (300 mLd^{-1}) conditions harvested after 45 d. The orange line represents a severe drought treatment (no water for 1 week) for both genotypes. (B) The pair-wise differential expression comparisons (1 to 5) performed between plants at 45 d time point. The genotypic comparisons are represented by blue bars. The number of genes differentially expressed (induced or repressed) at 1 % False Discovery Rate are indicated in green font for each of the comparisons. Complete lists as well as the 1 week comparisons are provided as supplemental data.

Figure 2. Brassinosteroid pathway. Sterol and brassinosteroid biosynthesis pathway is differentially regulated between the wild type and $P_{\text{SARK}}::\text{IPT}$. (A) Heat map of a selected set of BR-related genes derived from hierarchical cluster analysis. Red color represents higher relative expression and blue represents lower relative expression when compared to the mean expression value across all samples. Scale is the \log_2 of Mean expression values. Figure is representative of two independent experiments. (B) Validation of a subset of BR-related genes using q-PCR assay. WT plants growing under control conditions (1000 mLd^{-1}) were used as reference sample ($\log_2=0$). Each data point represents the Mean \pm SE ($n=6$). Two internal controls (rRNA 18S and UBQ2) were used for data normalization. FACKEL (HYD2), Cyclopropyl isomerase (CPI1), Sterol-4-Alpha methyl oxidase 1-1 (SMO1-1), Sterol methyl transferase 2 (SMT2), Farnesyl diphosphate synthase 1 (FPS1), Brassinosteroid insensitive 2 (BIN2), C-5 sterol desaturase

(DWARF7), DWARF1/DIMINUTO1, Brassinosteroid-6-oxidase 1, Brassinosteroid-responsive ring H2 (BRH1), Arabidopsis Shaggy-related protein kinase DZETA (ASKDZETA).

Figure 3. Tetrapyrrole Expression Cluster. Heat map of a selected set of tetrapyrrole-related genes derived from hierarchical cluster analysis. Red color represents higher relative expression and blue represents lower relative expression when compared to the mean expression value across all samples. Scale is the \log_2 of Mean expression values. The set of tetrapyrrole synthesis-related genes represented on the array were differentially regulated between the WT and *P_{SARK}::IPT* plants. Almost all the genes associated with the tetrapyrrole pathway had higher transcript abundance in the *P_{SARK}::IPT* plants. Figure is representative of three independent experiments.

Figure 4. MapMan illustration of enriched pathways. Array expression data was imported into the MapMan software. Several pathways showed striking enrichment: Light reactions, Calvin-Benson cycle, and photorespiration when both genotypes were exposed to a reduced watering regime. Red color in square boxes represents up-regulation and blue represent repressed expression in *P_{SARK}::IPT* plants when compared to WT. Each data point corresponds with the \log_2 of the Mean value from 3 biological replicates.

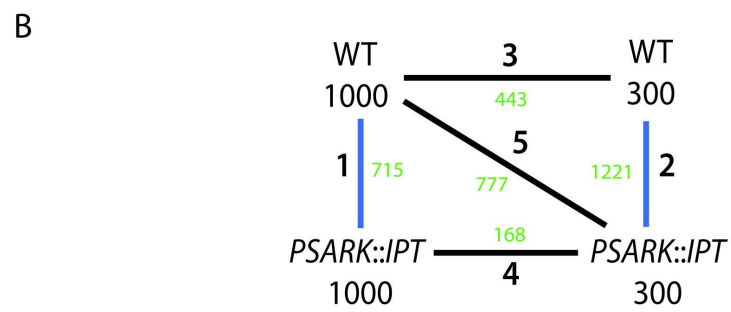
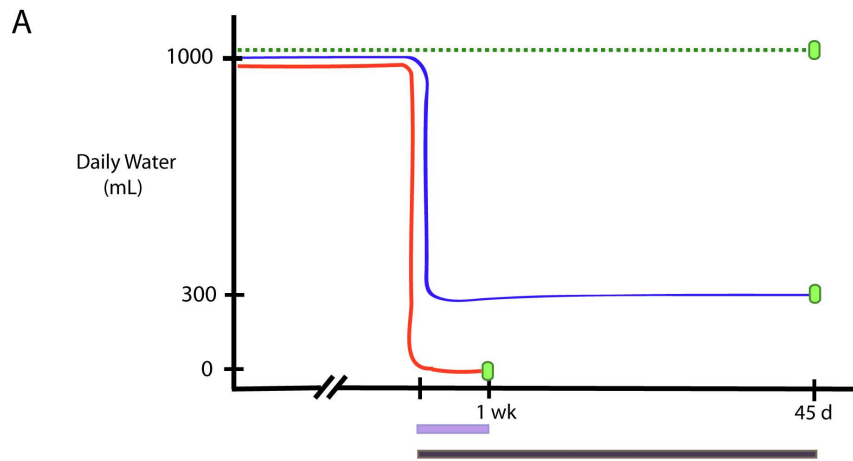
Figure 5. Analysis of genes associated with the photosynthesis complexes. (A) Classification and differential expression (\log_2) of photosynthesis-related genes. The analysis of the DNA microarrays was performed as described in Materials and Methods section for 3 biological replicates. (B) Validation of the microarray expression by qPCR. WT plants growing under control conditions (1000 mLd⁻¹) was used as reference sample ($\log_2=0$). Each data point

represents the Mean \pm SE (n=6). Two internal controls (rRNA 18S and UBQ2) were used for the data normalization.

Figure 6. Photosynthesis-related protein expression. (A) SDS-PAGE gel staining. The different protein samples were normalized according to their chlorophyll content. A total of 0.5 μ g of chlorophyll were loaded in each lane. (B) Western blots of the different protein samples were probed with antibodies raised against D1, D2, OEC, cyt b6/f, Fd, α -ATPase and PsaB. Quantification of each band was performed using ImageQuant software. Each value represents the Mean \pm SE (n=4). Samples were numbered as follows: 1. WT growing with 1000 mLd⁻¹; 2. WT growing with 300 mLd⁻¹; 3. *P_{SARK}::IPT* growing with 1000 mL d⁻¹; 4. *P_{SARK}::IPT* growing with 300 mLd⁻¹.

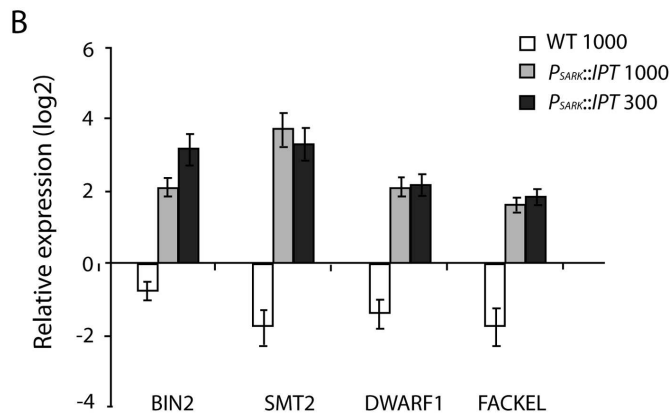
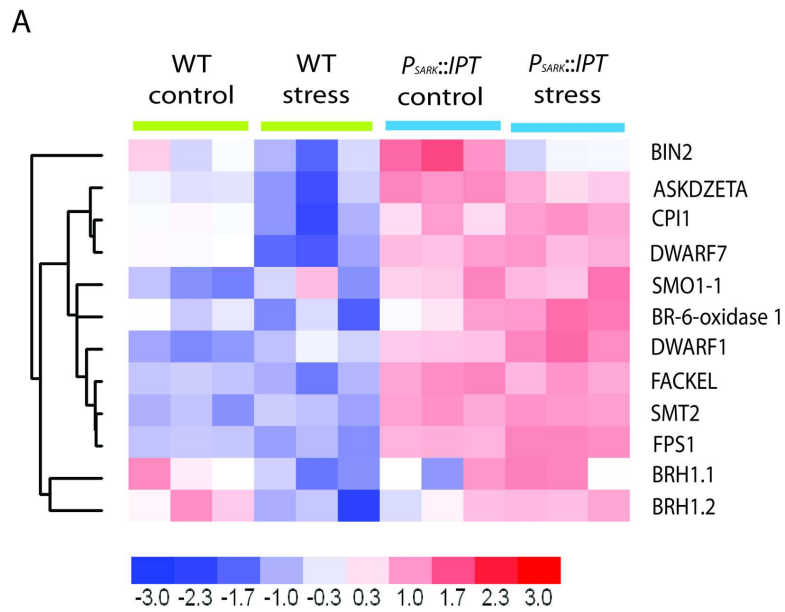
Figure 7. Changes in chlorophyll fluorescence during water deficit. (A) Photochemical quenching (qP); (B) non-photochemical quenching (NPQ) and (C) linear electron transport rate (ETR) measured by variation in chlorophyll fluorescence of WT and *P_{SARK}::IPT* plants growing under control conditions (1000 mL d⁻¹, filled symbols) or under water-restricted conditions (300 mL d⁻¹, open symbols). All measurements were performed as described in Materials and Methods. Each data point represents the Mean \pm SE (n=12).

Figure 1



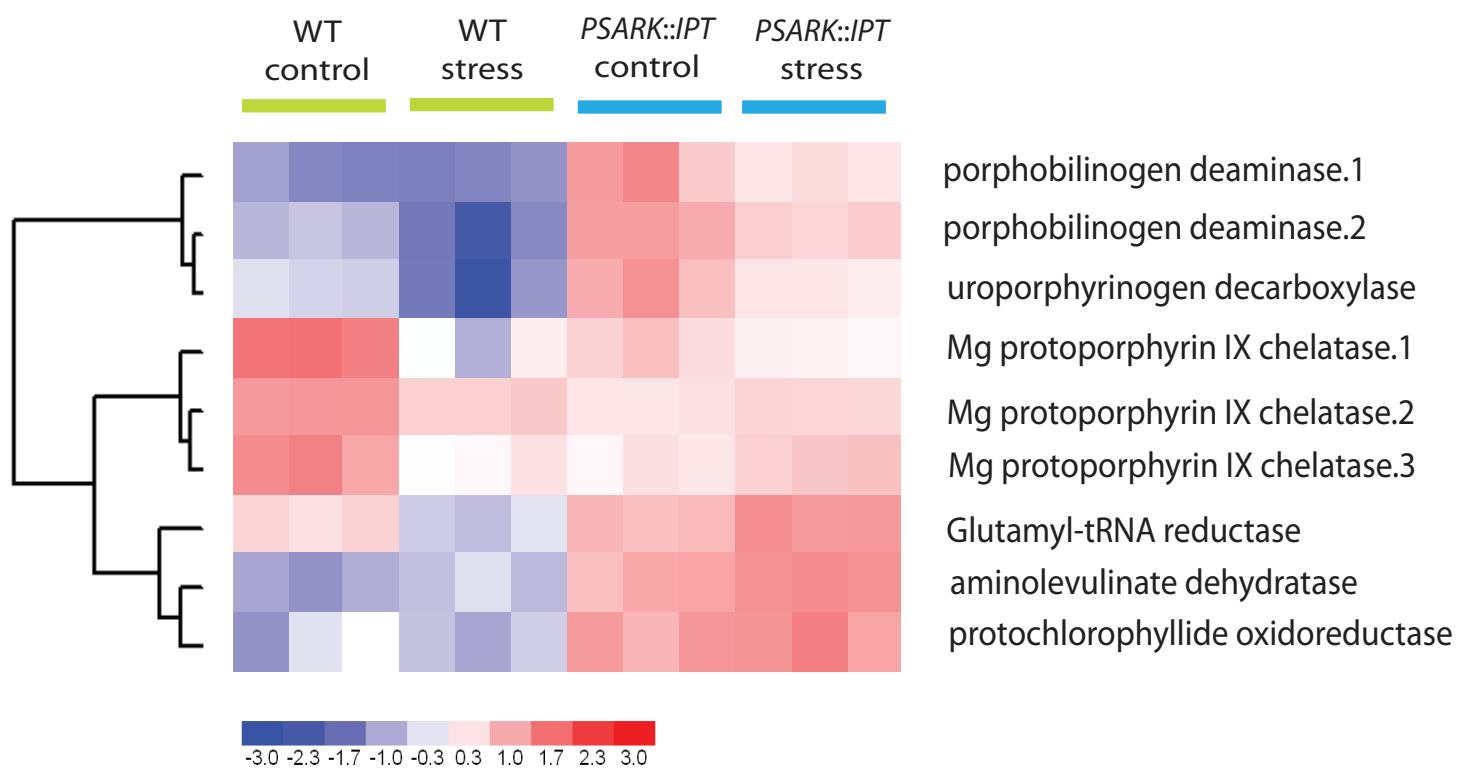
182x188mm (300 x 300 DPI)

Figure 2



139x214mm (300 x 300 DPI)

Figure 3



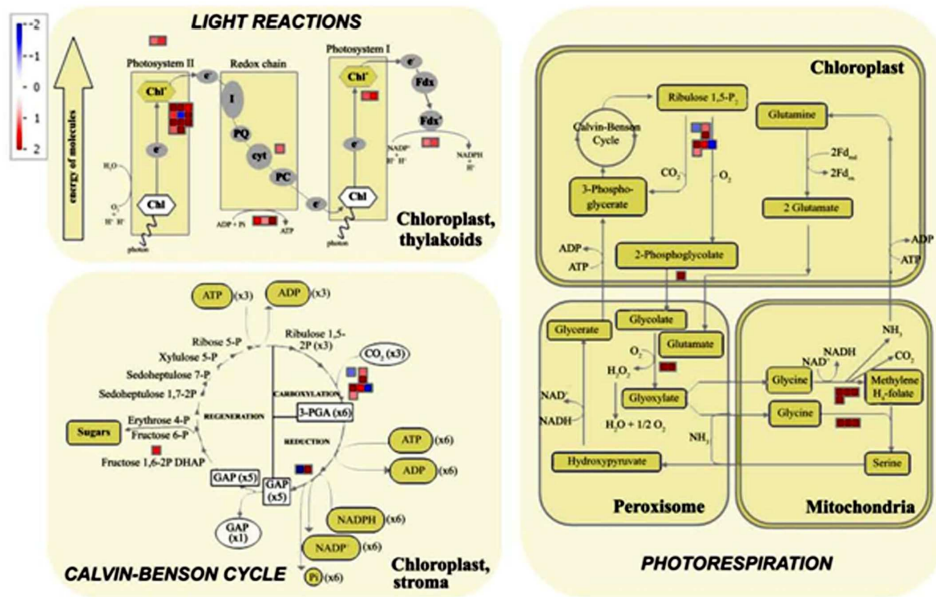


Figure 4
381x257mm (300 x 300 DPI)

A

Photosynthetic complex	Gene	Accession #	1	2	3	4
Antenna	Lhcb2	Les.147.1.S1_at	*	-2.02	1.65	1.12
	Lhcb4	Les.3297.2.S1_at	-1.27	*	1.1	*
	Lhcb5	Les.2286.1.S1_at	*	-1.23	1.38	1.35
	Lhcb6	Les.4492.2.S1_at	*	-1.23	*	*
Photosystem II	PsbT	Les.3063.1.S1_at	*	-2.02	1.69	2.24
	PsbX	Les.5812.1.S1_at	1.07	*	3.32	2.15
		Les.2377.2.A1_at	*	*	*	2.56
		Les.2377.1.S1_at	*	*	*	1.99
	PsbW	Les.4586.1.S1_at	*	-2.55	1.96	1.66
		Les.2620.2.S1_at	*	*	*	1.35
		LesAffx.70106.2.S1_at	0.97	-1.44	2.32	2.09
	PsbP	LesAffx.70106.1.S1_at	*	*	*	3.44
		Les.1923.1.S1_at	*	*	*	1.43
		LesAffx.66410.1.S1_at	*	-2.43	1.07	*
	PsbC	LesAffx.65143.1.S1_at	*	*	*	*
	PsbF	LesAffx.67937.1.S1_at	*	-2.12	2.66	2.18
OEC	Les.4821.S1_at	*	*	*	1.19	
Cytochrome b6/f	PetB	LesAffx.51226.1A1_at	1.66	-2.33	2.31	1.16
	PetA	LesAffx.30946.1.S1_at	*	*	*	*
	PetM	Les.3087.2.S1_at	1.07	*	*	*
Photosystem I	PsaN	Les.2168.1.S1_at	1.86	-3.02	3.33	1.24
	PsaO	Les.4508.1.S1_at	*	*	1.17	*
	PsaH	Les.3170.2.S1_at	*	-2.13	2.27	1.53
NAD(P)H Oxidoreductase	Oxidoreductase	Les.2074.1.A1_at	*	-3.21	1.55	1.07
	PetH	Les.3287.1.S1_at	*	-1.57	1.65	1.27
	PetJ	LesAffx.5776.S1_at	*	-1.55	1.44	1.69
ATP Synthase	α -ATPase	Les.4995.1.S1_atq	*	-3.03	1.77	1.59
	δ -ATPase	Les.4867.1.S1_at	*	-2.56	2.09	1.02
	β -ATPase	Les.1260.1.S1_at	2.51	-1.58	*	*
	γ -ATPase	Les.4615.1.S1_at	*	-3.76	1.97	2.80

1. $P_{SARK}::IPT$ 1000 mL vs. WT 1000 mL 3. $P_{SARK}::IPT$ 300 mL vs. WT 1000 mL *: not significant differences
 2. WT 300 vs. WT 1000 mL 4. $P_{SARK}::IPT$ 300 vs. WT 300 mL

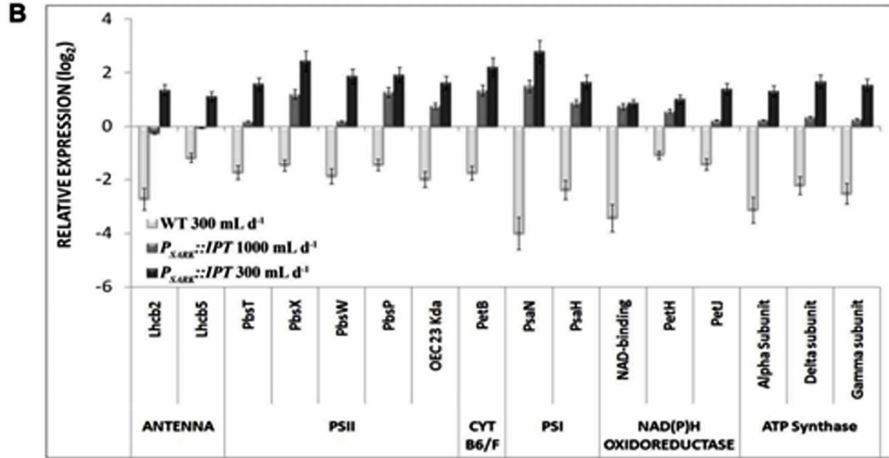


Figure 5
 152x197mm (300 x 300 DPI)

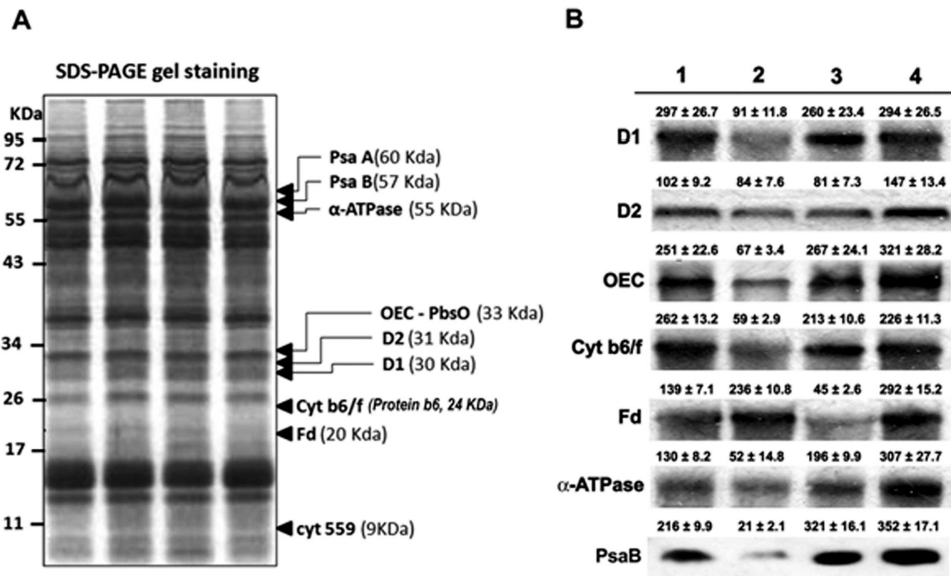


Figure 6
203x125mm (300 x 300 DPI)

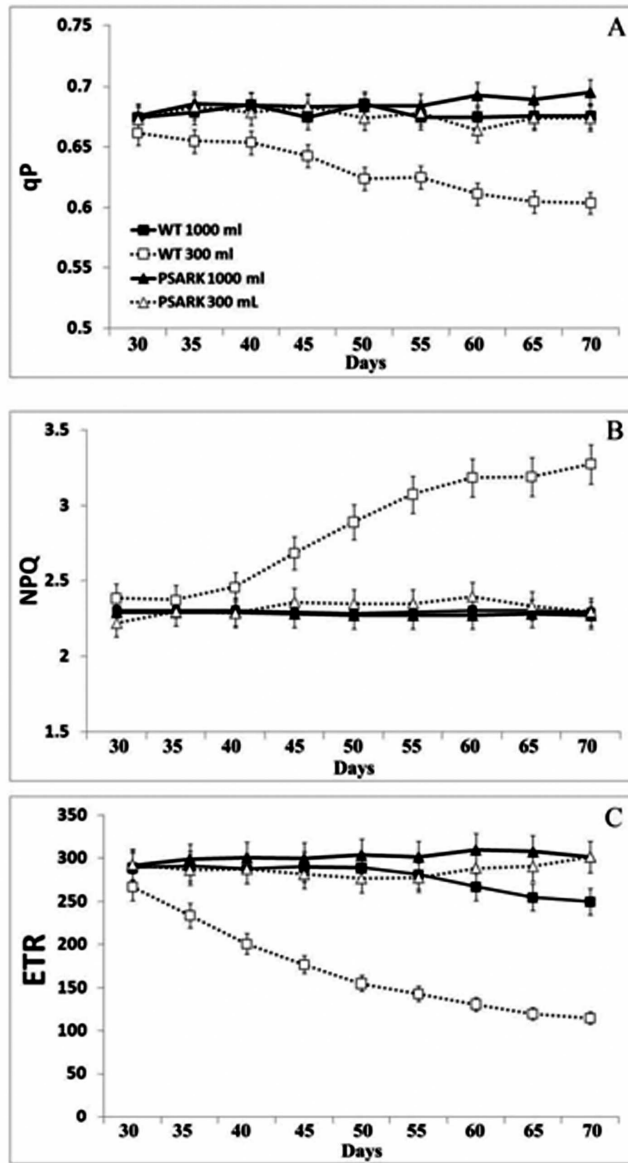


Figure 7
254x446mm (300 x 300 DPI)